Polynuclear Gold Complexes with Bridging Selenido Ligands. Theoretical Studies of Gold−Gold Interactions

Silvia Canales,[†] Olga Crespo,[†] M. Concepción Gimeno,[†] Peter G. Jones,[‡]
Antonio Laguna,*,[†] and Fernando Mendizabal[§]

Departamento de Química Inorgánica, Instituto de Ciencia de Materiales de Aragón,
Universidad de Zaragoza-CSIC, E-50009 Zaragoza, Spain, and Institut für Anorganische
und Analytische Chemie der Technischen Universität, Postfach 3329,
D-38023 Braunschweig, Germany, and Facultad de Ciencias, Universidad de Chile,
Casilla 653, Santiago de Chile, Chile

The compounds [Se(AuPPh$_3$)$_2$] and [Se(Au$_2$dppf)] are good precursors for the synthesis of highly aurated selenium-centered derivatives. Thus the reaction of [Se(AuPPh$_3$)$_2$] with various molar ratios of [Au(OTf)PPh$_3$] affords the homoleptic species [Se(AuPPh$_3$)$_n$](OTf)$_{n-2}$ ($n = 3-6$). Similarly, the treatment of [Se(Au$_2$dppf)] with various stoichiometric ratios of [Au$_2$(OTf)$_2$(μ-dppf)] gives the polynuclear derivatives [(Au$_2$dppf){Se(Au$_2$dppf)}$_2$](OTf)$_2$, [Se(Au$_2$dppf)$_2$](OTf)$_2$, and [Se(Au$_2$dppf)$_3$](OTf)$_4$. The compounds [Au{Se(AuPPh$_3$)$_2$}$_2$]ClO$_4$ and [Au{Se(Au$_2$dppf)}$_2$]ClO$_4$ have been obtained by reaction of the precursors with [Au(tht)$_2$]-ClO$_4$ in a molar ratio of 2:1. Some of these derivatives have been characterized by X-ray diffraction studies and show unusual geometries, associated with gold−gold interactions. The latter have been studied theoretically using [Se(AuPH$_3$)$_n$]$^{(n-2)+}$ ($n = 2-6$) models at the HF and MP2 levels with quasi-relativistic pseudopotentials. There is a good agreement between experimental and theoretical geometries.

Introduction

In the past few years a great deal of attention has been paid to the chemistry of polynuclear gold derivatives with a central heteroatom, not only from the experimental and structural but also from the theoretical standpoint.[1] Interesting hypercoordinated species of the type [C(AuPR$_3$)$_5$]$^+$, [C(AuPR$_3$)$_6$]$^{2+}$, [N(AuPR$_3$)$_5$]$^{2+}$, [P(AuPR$_3$)$_5$]$^{2+}$, and [P(AuPR$_3$)$_6$]$^{3+}$ have been described,[2] apart from other complexes with more conventional stoichiometry, and all have in common the presence of gold−gold interactions of ca. 3 Å. Usually, the chemistry of the first-row elements of the p-block is known to follow classical rules of bonding, and only in cases of extreme electron deficiency does the traditional electron count need to be reconsidered to account for special types of molecular or solid state structures. Many of these heteroatom-centered complexes are electron-deficient, and the gold−gold interactions provide a significant contribution to their stability.

The attraction between these closed-shell systems has recently captured attention in inorganic and organo-metallic chemistry.[1] P. Pyykkö has summarized the available theoretical and experimental evidence of intra- and intermolecular interactions between heavy metal atoms, such as Au(I).[3] In general, when heavy metals are involved in such interactions, the closed-shell attractions are of metallophilic or van der Waals type, as has been found for d^8, d^{10} coinage-metals, and d^{10}s^2 centers. Experimental evidence for the aurophilic Au-(I)- - -Au(I) attraction is available from crystallography, NMR and Raman spectroscopies, and optical spectroscopic measurements of the interaction strength.[4] It is manifested in molecular conformations with relatively close Au- - -Au interactions of ca. 3 Å, whose strength has been estimated at ca. 33 kJ/mol.[5] These attractions are weaker than most covalent or ionic bonds, but stronger than other van der Waals bonds and comparable in strength to typical hydrogen bonds. The phenomenon cannot be satisfactorily explained by classical theories such as hybridization.[3]

From a theoretical point of view, the attractions close to equilibrium distances are caused by dispersive in-

† Universidad de Zaragoza-CSIC.
‡ Institut für Anorganische und Analytische Chemie der Technischen Universität Braunschweig.
§ Universidad de Chile.
(1) (a) Schmidbaur, H. *Chem. Soc. Rev.* **1995**, 391. (b) Laguna, A. In *Gold, Progress in Chemistry, Biochemistry and Technology,* Inter-national; Schmidbaur, H., Ed.; Wiley: New York, 1999. (c) Schmidbaur, H. *Pure Appl. Chem.* **1993**, *65*, 691.
(2) (a) Scherbaum, F.; Grohmann, A.; Müller, G.; Schmidbaur, H. *Angew. Chem., Int. Ed. Engl.* **1989**, *28*, 463. (b) Scherbaum, F.; Grohmann, A.; Huber, B.; Krüger, C.; Schmidbaur, H. *Angew. Chem., Int. Ed. Engl.* **1988**, *27*, 1544. (c) Grohmann, A.; Riede, J.; Schmidbaur, H. *Nature* **1990**, *345*, 140. (d) Schmidbaur, H.; Weidenhiller, G.; Steigelmann, O. *Angew. Chem., Int. Ed. Engl.* **1991**, *30*, 433. (e) Zeller, E.; Schmidbaur, H. *J. Chem. Soc., Chem. Commun.* **1993**, 69.

(3) Pyykkö, P. *Chem. Rev.* **1997**, *97*, 597.
(4) (a) Jones, P. G. *Gold Bull.* **1981**, *14*, 102. (b) Schmidbaur, H. *Gold Bull.* **1990**, *23*, 11. (c) Gade, L. H. *Angew. Chem., Int. Ed. Engl.* **1997**, *36*, 1171. (d) Mansour, M. A.; Connick, W. B.; Lachicotte, R. J.; Gysling, H. J.; Eisenberg, R. J. *J. Am. Chem. Soc.* **1998**, *120*, 1329. (e) Canales, F.; Gimeno, M. C.; Laguna, A.; Jones, P. G. *J. Am. Chem. Soc.* **1996**, *118*, 4839.
(5) (a) Dziwok, K.; Lachmann, J.; Wilkinson, D. L.; Müller, G.; Schmidbaur, H. *Chem. Ber.* **1990**, *123*, 423. (b) Schmidbaur, H.; Graf, W.; Müller, G. *Angew. Chem., Int. Ed. Engl.* **1988**, *27*, 417. (c) Narayanaswamy, R.; Young, M. A.; Parkhurst, E.; Ouellette, M.; Kerr, M. E.; Ho, D. M.; Elder, R. C.; Bruce, A. E.; Bruce, M. R. M. *Inorg. Chem.* **1993**, *32*, 2506. (d) Harwell, M. E.; Mortimer, M. D.; Knobler, C. B.; Anet, F. A. L.; Hawthorne, M. F. *J. Am. Chem. Soc.* **1996**, *118*, 2679.

Scheme 1[a]
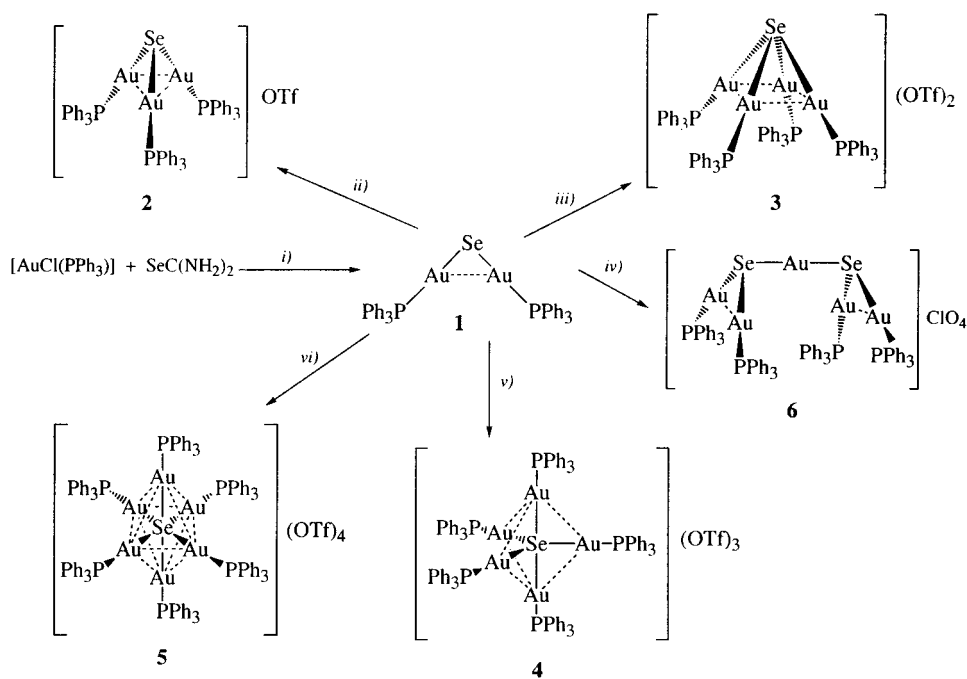
[a] (i) Na$_2$CO$_3$, MeOH, (ii) [Au(OTf)PPh$_3$], (iii) 2 [Au(OTf)PPh$_3$], (iv) 1/2 [Au(tht)$_2$]ClO$_4$, (v) 3 [Au(OTf)PPh$_3$], (vi) 4 [Au(OTf)PPh$_3$].

teractions together with relativistic effects.[6] The attractive contributions are dominated by pair-excitations from the heavy metal, such as gold 5d, strengthened by relativistic effects. In all the cases where there are inter- or intramolecular metal–metal attractions, the correlation effects are essential; if they are omitted, at the Hartree–Fock (HF) level, repulsive interactions are obtained.[6] Hence, it is necessary to use at least second-order Møller–Plesset level (MP2) methods for the dispersive forces, which are included in the electronic correlation effects.[7]

Although the chemistry of carbon-, nitrogen-, phosphorus-, or arsenic-centered species has developed rapidly, the corresponding chemistry of chalcogen derivatives is still growing. We have previously reported the synthesis and structural characterization of sulfur-centered complexes,[4e,8] and here we describe the synthesis of polynuclear gold complexes with selenium as the central heteroatom. We have also studied theoretically the gold–gold interactions in these complexes. The synthesis of the compound [Se(AuPPh$_3$)$_4$](OTf)$_2$ with a quadruply bridging selenido ligand has been the subject of a preliminary communication.[9]

Results and Discussion

We have previously reported that the sulfur derivatives [S(AuPR$_3$)$_2$][10] or [S(Au$_2$dppf)] (dppf = 1,1′-bis-(diphenylphosphino)ferrocene)[4e] are excellent starting materials for the synthesis of highly aurated homoleptic sulfur-centered derivatives. Our aim was to obtain similar complexes with selenium as central element. The complex [Se(AuPPh$_3$)$_2$] **1** was prepared in high yield by reacting [AuCl(PPh$_3$)] with selenourea followed by basic hydrolysis.[11] We have studied further auration around the selenium center by reaction of **1** with various stoichiometric ratios of [Au(OTf)PPh$_3$] to give the trinuclear [Se(AuPPh$_3$)$_3$]OTf **2**, tetranuclear [Se(AuPPh$_3$)$_4$](OTf)$_2$ **3**, pentanuclear [Se(AuPPh$_3$)$_5$](OTf)$_3$ **4**, or hexanuclear [Se(AuPPh$_3$)$_6$](OTf)$_4$ **5** species (see Scheme 1).

The products are air-stable colorless solids, insoluble in nonpolar solvents, and readily soluble in dichloromethane or chloroform. The conductivities of the complexes measured in acetone are in agreement with the proposed formulas. Although there is not many data for conductivities of highly charged compounds, the tri- and tetracationic species show values similar to those found in the sulfur-centered complexes.[8b]

The ^{31}P(^{1}H) NMR spectra for complexes **1**−**5** show a sharp single resonance, indicating the equivalence of all the phosphine groups. The variable-temperature experiments confirm that all the AuPR$_3^+$ fragments are equivalent, maybe because of a rapid exchange in solution even at low temperature. An upfield displacement is observed when a new gold fragment coordinates to the selenium center. We have previously observed this upfield shift in the sulfur derivatives.[8b]

The structure of the [Se(AuPPh$_3$)$_3$]$^+$ unit is known and is analogous to that in the oxonium and sulfonium salts

(6) (a) Pyykkö, P.; Zhao, Y.-F. *Angew. Chem.* **1991**, *103*, 622. (b) Pyykkö, P.; Li, L.; Runenberg, N. *Chem. Phys. Lett.* **1994**, *218*, 133. (c) Pyykkö, P.; Mendizabal, F. *Inorg. Chem.* **1998**, *37*, 3018. (d) Runenberg, N.; Schütz, M.; Werner, H.-J. *J. Chem. Phys.* **1999**, *110*, 7210. (e) Pyykkö, P.; Schneider, W.; Bauer, A.; Bayler, A.; Schmidbaur, H. *Chem. Commun.* **1997**, 1111.

(7) Møller, C.; Plesset, M. S. *J. Chem. Phys.* **1934**, *46*, 618.

(8) (a) Canales, F.; Gimeno, M. C.; Jones, P. G.; Laguna, A. *Angew. Chem., Int. Ed. Engl.* **1994**, *33*, 769. (b) Canales, F.; Gimeno, M. C.; Laguna, A.; Villacampa, M. D. *Inorg. Chim. Acta* **1996**, *244*, 95. (c) Canales, F.; Gimeno, M. C.; Laguna, A.; Jones, P. G. *Organometallics* **1996**, *15*, 3412. (d) Calhorda, M. J.; Canales, F.; Gimeno, M. C.; Jiménez, J.; Jones, P. G.; Laguna, A.; Veiros, L. F. *Organometallics* **1997**, *16*, 3837. (e) Canales, F.; Canales, S.; Crespo, O.; Gimeno, M. C.; Jones, P. G.; Laguna, A. *Organometallics* **1998**, *17*, 1617.

(9) Canales, S.; Crespo, O.; Gimeno, M. C.; Jones, P. G.; Laguna A. *J. Chem. Soc., Chem. Commun.* **1999**, 679.

(10) Lensch, C.; Jones, P. G.; Sheldrick, G. M. *Z. Naturforsch., Teil B* **1982**, *37b*, 944.

(11) Jones, P. G.; Thöne, C. *Chem. Ber.* **1991**, *124*, 2725.

Scheme 2[a]
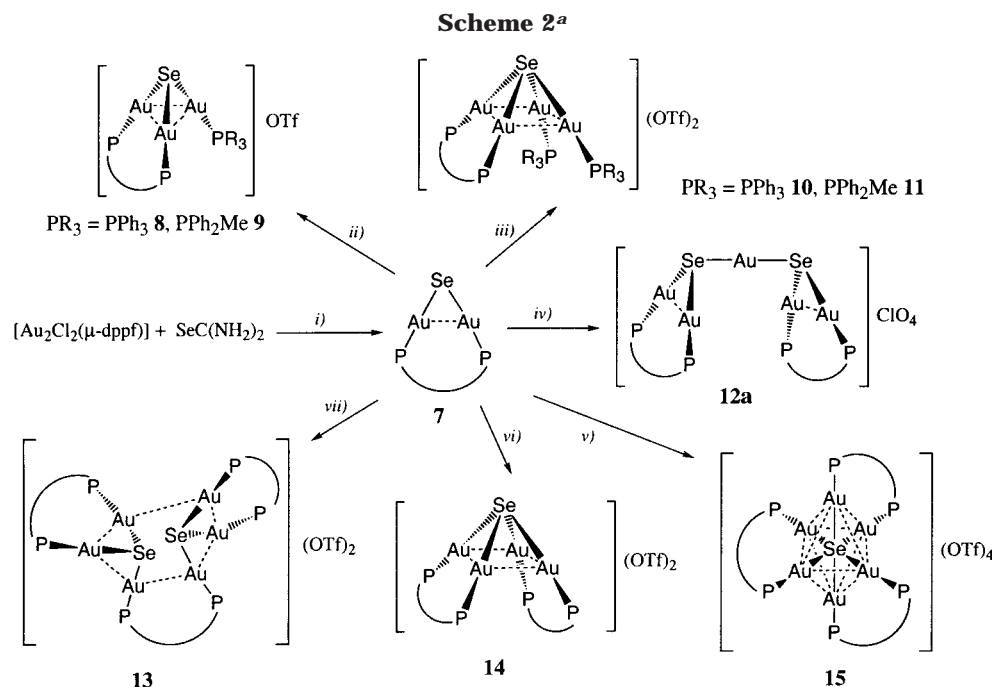
[a](i) Na_2CO_3, MeOH, (ii) [Au(OTf)PPh$_3$] or [Au(OTf)PPh$_2$Me], (iii) 2 [Au(OTf)PPh$_3$] or 2 [Au(OTf)PPh$_2$Me], (iv) 1/2 [Au(tht)$_2$]ClO$_4$, (v) 2 [Au$_2$(OTf)$_2$(μ-dppf)], (vi) [Au$_2$(OTf)$_2$(μ-dppf)], (vii) 1/2 [Au$_2$(OTf)$_2$(μ-dppf)].

and consists of trigonal pyramids with basal gold atoms and selenium at the apex.[10] The synthesis and structural characterization of the tetragold species has been previously communicated by us;[9] the structure shows a square pyramidal geometry with the selenium atom in the apical position and in the base the four gold atoms forming short gold–gold interactions. We believe that the structures of the complexes with five and six gold atoms could be trigonal pyramidal and octahedral, respectively, with close gold–gold distances. The high charge of the cations has however prevented the growth of single crystals for an unambiguous determination.

The reaction of **1** with [Au(tht)$_2$]ClO$_4$ in a molar ratio of 2:1 leads to the pentanuclear complex [Au{Se-(AuPPh$_3$)$_2$}$_2$] **6**. Complex **6** is an air-stable white solid that behaves as a 1:1 electrolyte in acetone solutions. The ^{31}P(^{1}H) NMR spectrum presents one singlet for all phosphorus atoms even at low temperature. In the positive-ion liquid secondary mass spectrum (LSIMS) the cation molecular peak appears at $m/z = 2193$ (15%) with coincident experimental and isotopic distribution.

Treatment of [Au$_2$Cl$_2$(μ-dppf)] with selenourea followed by basic hydrolysis affords the complex [Se(Au$_2$-dppf)] **7**, in which the two gold atoms are bridged by the 1,1′-bis(diphenylphosphino)ferrocene ligand and the selenium atom. Complex **7** is an orange air-stable solid that is nonconducting in acetone solutions.

The NMR data are consistent with the formulation, and only one signal is observed in the ^{31}P(^{1}H) NMR spectrum, because of the equivalence of both phosphorus atoms. In the ^{1}H NMR spectrum, apart from the multiplets for the phenyl protons, two broad multiplets appear for the α and β protons of the cyclopentadienyl rings. The low-temperature spectrum presents four signals for the cyclopentadienyl protons, which is a typical behavior of 1,1′-disubstituted ferrocene derivatives; the protons are strictly not equivalent but are rendered so by fluxionality processes. Up to eight signals
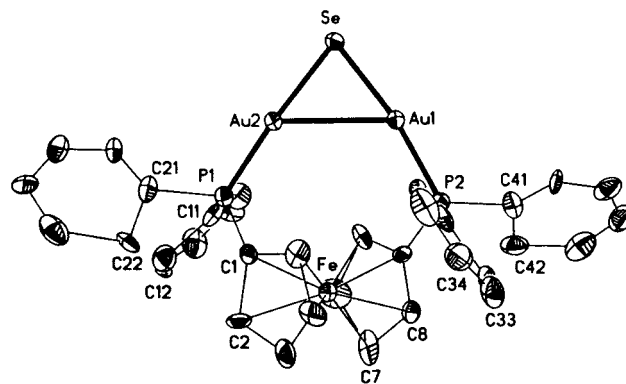
Figure 1. Structure of complex **7** in the crystal with the atom-numbering scheme. Displacement parameter ellipsoids represent 50% probability surfaces. The H atoms are omitted for clarity.

Table 1. Selected Bond Lengths [Å] and Angles [deg] for Compound 7

Au(1)–P(2)	2.263(3)	Au(2)–P(1)	2.254(3)
Au(1)–Se	2.4218(11)	Au(2)–Se	2.4055(11)
Au(1)–Au(2)	2.9353(8)		
P(2)–Au(1)–Se	175.47(8)	C(8)–P(1)–Au(2)	109.1(3)
P(2)–Au(1)–Au(2)	124.64(7)	C(21)–P(1)–Au(2)	112.9(3)
Se–Au(1)–Au(2)	52.30(3)	C(11)–P(1)–Au(2)	119.1(3)
P(1)–Au(2)–Se	170.67(7)	C(3)–P(2)–Au(1)	112.9(3)
P(1)–Au(2)–Au(1)	117.93(7)	C(31)–P(2)–Au(1)	113.2(3)
Se–Au(2)–Au(1)	52.80(3)	C(41)–P(2)–Au(1)	117.2(3)
Au(2)–Se–Au(1)	74.90(3)		

are observed in the low-temperature spectra of these derivatives. The LSIMS shows the molecular peak at $m/z = 1028$ (87%).

The crystal structure of complex **7** has been determined by X-ray diffraction studies, and the molecule is shown in Figure 1. Selected bond lengths and angles are collected in Table 1. The selenido ligand is bonded to the gold atoms of an "Au$_2$(μ-dppf)" unit with a gold–gold contact of 2.9353(8) Å. This value is shorter than

that found for $[Se(AuPPh_3)_2]$ (3.051(1) Å).[11] An extreme distortion of ideal geometry at the selenium center [Au−Se−Au = 74.90(3)°] is observed, even more so than for $[Se(AuPPh_3)]$ [Au−Se−Au = 79.1(1)°].[11]

The presence in **7** of a bridging ligand, with less steric demand than two triphenylphosphine ligands, probably allows a shorter gold−gold contact and a more pronounced narrowing of the angle at selenium. The same effects are observed in $[S(Au_2dppf)]$[4e] (shorter gold−gold contact and more narrowing) related to $[S(AuPPh_3)_2]$.[10] A comparison of **7** with $[S(Au_2dppf)]$ reveals a larger angle Au−E−Au (E = S, Se) for the sulfido ligand. This may be associated with the presence of more diffuse 4p orbitals in the selenium derivative or a greater electron repulsion of the lone pairs. The distortion of linear geometry in the gold atoms is more marked for Au(2) [P(1)−Au(2)−Se = 170.67(7)°] than for Au(1) [P(2)−Au-(1)−Se = 175.47(8)°]. The distances Au−Se (Au(1)−Se = 2.4218(11), Au(2)−Se = 2.4055(11) Å) are dissimilar but longer than those found for $[Se(AuPPh_3)_2]$ (2.394-(1), 2.398(1) Å).[11] The distances Au−P are also marginally dissimilar (Au(1)−P(2) = 2.263(3), Au(2)−P(1) = 2.254(3) Å); the shorter compares well with those in $[Se-(AuPPh_3)_2]$ (2.254(2), 2.255(2) Å).[11]

Complex **7** can serve as a building block for preparing polynuclear selenium-centered derivatives (Scheme 2). We have studied the reactions of **7** with several gold(I) compounds. Thus the treatment of **7** with 1 or 2 equiv of $[Au(OTf)PR_3]$ affords the complexes $[Se(Au_2dppf)-(AuPR_3)]OTf$ (PR$_3$ = PPh$_3$ **8**, PPh$_2$Me **9**) or $[Se(Au_2dppf)-(AuPR_3)_2](OTf)_2$ (PR$_3$ = PPh$_3$ **10**, PPh$_2$Me **11**). They behave as 1:1 or 1:2 electrolytes in acetone solution, respectively.

The ^1H NMR spectra show multiplets for the phenyl protons and two multiplets for the cyclopentadienyl protons; compounds **9** and **11** also present a doublet for the methyl group of the phosphine, the integral ratio agreeing with the proposed formulas. The $^{31}P(^1H)$ spectra show two signals because of the two different phosphorus environments. In the positive-ion liquid secondary mass spectra the cation molecular peaks, [M − OTf]$^+$, appear for complex **8** at m/z = 1486 (100%) and for compound **9** at m/z = 1425 (100%); for complex **10** the peak $[Se(Au_2dppf)(AuPPh_3)_2]^+$ appears at m/z = 1945, although with very low intensity, and is absent in the spectrum of complex **11**.

Although these complexes have not been characterized by X-ray diffraction, we assume that compounds **8** and **9** have a structural framework similar to that found in the complex $[Se(AuPPh_3)_3]^+$, with short contacts between the gold(I) centers, whereas **10** and **11** could have a structure similar to $[Se(AuPPh_3)_4]^{2+}$.

In the mass spectra of these selenium-centered derivatives the fragment corresponding to the cation [Au{Se(Au$_2$dppf)}$_2$]$^+$ always appears with high intensity. This indicates the stability of this compound, and we have synthesized it by treatment of 2 equiv of [Se(Au$_2$-dppf)] with 1 equiv of [Au(tht)$_2$]ClO$_4$. The reaction leads to the compound [Au{Se(Au$_2$dppf)}$_2$]ClO$_4$ **12a** as an orange solid that behaves as a 1:1 electrolyte in acetone solution.

The NMR spectra at room temperature show broad bands for the cyclopentadienyl protons and a broad singlet for the phosphorus atoms; the low-temperature
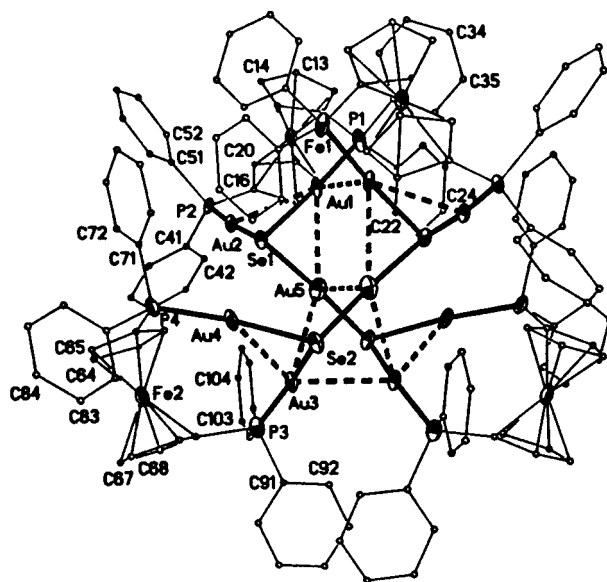
Figure 2. Structure of the cation of complex **12b**. Displacement parameter ellipsoids represent 50% probability surfaces. Carbon atoms are spheres of arbitrary radius. The H atoms are omitted for clarity.

spectrum is very complicated as a consequence of the inequivalence of all protons and phosphorus nucleus. In the ^1H NMR spectrum several signals appear in the region of the Cp protons, 16 in total, some of which are overlapped. The ^{31}P NMR spectrum presents four resonances for the four different phosphorus environments. In the positive-ion liquid secondary mass spectrum the cation molecular peak appears at m/z = 2251 (100%).

All attempts to crystallize complex **12a** failed, and then we added to a solution of complex **12a** another anion in order to get single crystals. We have determined the crystal structure of this complex with the anion NO$_3^-$ (Figure 2), **12b**; a selection of bond lengths and angles are collected in Table 2. The structure displays two [Au{Se(Au$_2$dppf)}$_2$]$^+$ moieties joined through gold−gold interactions and related by crystallographic 2-fold symmetry. There are several gold−gold contacts in the range 2.908(4)−3.182(3) Å; the shortest is between the gold atoms bridging the [Se(Au$_2$dppf)] units, Au(5)−Au(5)# 2.908(4) Å (# −x+1, y, −z+1/2). The selenium atoms act as triply bridging ligands with dissimilar distances to the gold atoms; for the gold atoms in the [Se(Au$_2$dppf)] units the distances are of the same order, 2.426(4)−2.462(4) Å, and are shorter for the gold atoms bridging these units, 2.396(4) and 2.398(4) Å; this is presumably attributable to the greater trans influence of P donors. The latter is similar to the shorter distance found in complex **7** (with a two-coordinate selenium donor atom) and the former to those in $[Se(AuPPh_3)_3]PF_6$. The angles around the selenium atoms are very irregular; those in the [Se(Au$_2$dppf)] units are narrower, 74.33(11)° and 75.21(11)°. All the gold atoms display a slightly distorted linear geometry (ignoring the gold−gold contacts).

We have also synthesized a hexanuclear derivative that contains two SeAu$_3$ cores connected through a bridging dppf ligand. The reaction of complex **7** with a freshly prepared solution of [Au$_2$(OTf)$_2$(μ-dppf)] in dichloromethane (molar ratio 2:1) affords [(Au$_2$dppf){Se(Au$_2$-

Table 2. Selected Bond Lengths [Å] and Angles [deg] for Compound 12b[a]

Au(1)−P(1)	2.291(10)	Au(3)−Au(4)	2.960(2)
Au(1)−Se(1)	2.465(4)	Au(3)−Au(3)#1	3.015(3)
Au(1)−Au(1)#1	2.920(3)	Au(3)−Au(5)	3.182(3)
Au(1)−Au(2)	2.985(2)	Au(4)−P(4)	2.255(10)
Au(1)−Au(5)	3.041(3)	Au(4)−Se(2)	2.437(4)
Au(2)−P(2)	2.264(10)	Au(5)−Se(2)#1	2.396(4)
Au(2)−Se(1)	2.426(4)	Au(5)−Se(1)	2.398(4)
Au(3)−P(3)	2.278(10)	Au(5)−Au(5)#1	2.908(4)
Au(3)−Se(2)	2.462(4)		
P(1)−Au(1)−Se(1)	172.1(3)	Au(4)−Au(3)−Au(5)	85.37(6)
P(1)−Au(1)−Au(1)#1	99.1(2)	Au(3)#1−Au(3)−Au(5)	70.38(4)
Se(1)−Au(1)−Au(1)#1	88.67(10)	P(4)−Au(4)−Se(2)	174.4(3)
P(1)−Au(1)−Au(2)	120.3(2)	P(4)−Au(4)−Au(3)	123.7(3)
Se(1)−Au(1)−Au(2)	51.80(9)	Se(2)−Au(4)−Au(3)	53.22(10)
Au(1)#1−Au(1)−Au(2)	139.91(6)	Se(2)#1−Au(5)−Se(1)	175.44(15)
P(1)−Au(1)−Au(5)	130.5(3)	Se(2)#1−Au(5)−Au(5)#1	95.73(11)
Se(1)−Au(1)−Au(5)	50.33(10)	Se(1)−Au(5)−Au(5)#1	88.21(11)
Au(1)#1−Au(1)−Au(5)	89.88(4)	Se(2)#1−Au(5)−Au(1)	129.78(12)
Au(2)−Au(1)−Au(5)	70.85(6)	Se(1)−Au(5)−Au(1)	52.30(10)
P(2)−Au(2)−Se(1)	175.6(2)	Au(5)#1−Au(5)−Au(1)	90.12(4)
P(2)−Au(2)−Au(1)	122.6(2)	Se(2)#1−Au(5)−Au(3)	81.17(11)
Se(1)−Au(2)−Au(1)	52.99(9)	Se(1)−Au(5)−Au(3)	97.95(10)
P(3)−Au(3)−Se(2)	163.4(3)	Au(5)#1−Au(5)−Au(3)	71.71(5)
P(3)−Au(3)−Au(4)	119.5(2)	Au(1)−Au(5)−Au(3)	146.41(7)
Se(2)−Au(3)−Au(4)	52.45(9)	Au(5)−Se(1)−Au(2)	92.76(13)
P(3)−Au(3)−Au(3)#1	108.3(2)	Au(5)−Se(1)−Au(1)	77.38(11)
Se(2)−Au(3)−Au(3)#1	83.71(10)	Au(2)−Se(1)−Au(1)	75.21(11)
Au(4)−Au(3)−Au(3)#1	130.92(6)	Au(5)#1−Se(2)−Au(4)	111.04(17)
P(3)−Au(3)−Au(5)	106.7(3)	Au(5)#1−Se(2)−Au(3)	94.71(13)
Se(2)−Au(3)−Au(5)	87.81(11)	Au(4)−Se(2)−Au(3)	74.33(11)

[a] Symmetry transformation used to generate equivalent atoms: #1 −x+1, y, −z+1/2.

dppf)}₂](OTf)₂ **13**. Compound **13** is an orange solid that behaves as a 2:1 electrolyte in an acetone solution.

The room-temperature NMR spectra show broad bands that sharpen when the experiment is carried out at low temperature. The ^1H NMR spectrum shows five close multiplets for the Cp protons in a ratio of 4:4:8:4:4, although some of the resonances may be overlapped. The $^{31}P\{^1H\}$ NMR spectrum presents three different phosphorus environments (in each $SeAu_3P_3$ unit). The inequivalence of these phosphorus and hydrogen atoms could be a consequence of different gold−gold interactions, as mentioned for complex **12a**. In the positive-ion LSIMS spectrum the dication molecular peak appears at $m/z = 3154$ (61%).

The structure of complex **13** has been confirmed by an X-ray diffraction study, and the cation is shown in Figure 3. Selected bond lengths and angles are given in Table 3. Compound **13** crystallizes with four dichloromethane molecules. The structure of the cation consists of an Se_2Au_6 core that shows short intramolecular Au−Au interactions. These distances vary from 2.9028(5) to 3.4325(6) Å. The shortest contacts, Au(5)−Au(6) = 2.9028(5) Å, Au(3)−Au(6) = 2.9779(6) Å, and Au(3)−Au(4) = 3.0088(5) Å, involve gold atoms of the [Au₂-dppf]²⁺ fragment that are bonded to the same selenium atom. The selenium atoms lie 1.566 and 1.623 Å out of the planes formed by their gold neighbors. The Au−Se−Au angles are very different: at Se(1) two of the angles are ca. 86°, whereas Au(4)−Se(1)−Au(3) is 75.86(3)°; at Se(2) the values range from 72.43(3)° for Au(5)−Se(2)−Au(6) to 89.02(3)° for Au(5)−Se(2)−Au(2), in accordance with the longest contact value found for Au(5)−Au(2). The Au−P and Au−Se distances, which range from 2.259(3) to 2.280(3) Å and 2.4240(10) to 2.4704(10) Å, compare well with those found in [Se(AuPPh₃)₃]PF₆.[10] The gold atoms display distorted linear geometries with
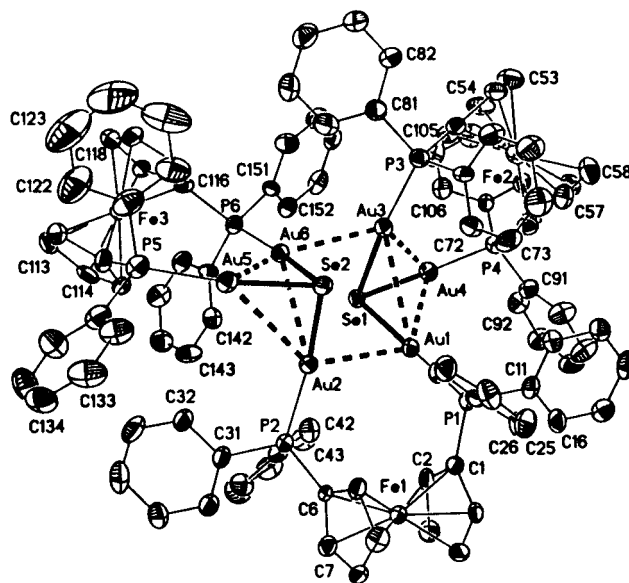

Figure 3. Perspective view of the cation of complex **13**. Displacement parameter ellipsoids represent 50% probability surfaces. The H atoms are omitted for clarity.

deviations from linearity [Se−Au−P from 174.68(7)° to 172.17(8)°] similar to those found in [Se(AuPPh₃)₃]PF₆ [Se−Au−P from 176.9(1)° to 172.7(1)°], except for Au-(2) [Se(2)−Au(2)−P(2) = 164.40(7)°], which shows considerable distortion.

Finally, we have studied the reaction of **7** with [Au₂-(OTf)₂(μ-dppf)] in 1:2 and 1:3 molar ratios to give the polynuclear derivatives [Se(Au₂dppf)₂](OTf)₂ **14** and [Se-(Au₂dppf)₃](OTf)₄ **15**. They are orange solids that show a conductivity value of a 1:2 electrolyte (**14**), and for **15** the value is similar to that obtained for compound **5**.

Complexes **14** and **15** show two broad resonances for

the cyclopentadienyl protons in the ^1H NMR spectra and one singlet for all the phosphorus atoms in the $^{31}P(^1H)$ NMR spectra. The low-temperature NMR spectra for complex **14** has been measured in $CDCl_3$ at -55 °C and in CD_2Cl_2 at -85 °C, and the results are similar. In the $^{31}P(^1H)$ NMR spectrum the singlet splits into several resonances, from which we have identified those belonging to complex **13**. We have observed that in this type of complex fast equilibrium processes are also present, and we accordingly believe that compound **14** could be in equilibrium with complex **13** and $[Au_2(OTf)_2(\mu\text{-dppf})]$ (see eq 1). For complex **15** the $^{31}P(^1H)$ NMR spectrum shows four signals; these can be attributed to different phosphorus environments and also to the presence of the *fac* and *mer* isomers.

(1)
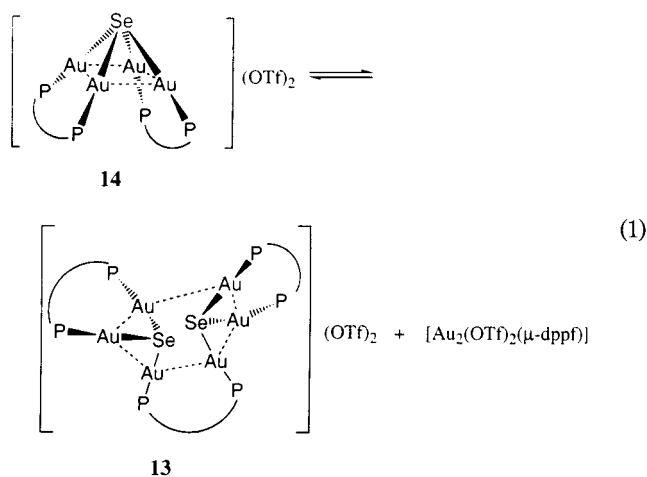
In the positive-ion liquid secondary mass spectrum (LSIMS+) of complex **14** the fragment corresponding to the molecular peak less a triflate anion appears, [Se-$(Au_2dppf)_2OTf]^+$, at $m/z = 1975$ (15%). For complex **15** the molecular peak does not appear probably due to the high charge, and only fragmentation peaks are observed.

The crystal structure of compound **14** has been studied by X-ray diffraction, but the results are made very imprecise by the presence of channels containing large amounts of solvent together with one triflate anion; no single chemical species could be identified in these channels. In view of this, we do not present full data. The cation is shown in Figure 4. Complex **14** crystallizes in the monoclinic space group $P2_1/n$ with unit cell dimensions $a = 17.3845$, $b = 15.2513$, $c = 33.1138$ Å, $\beta = 97.478°$. The structure is similar to that found for $[Se(AuPPh_3)_4](OTf)_2$.[9] The gold atoms in the $SeAu_4$ core exhibit gold–gold interactions that range from 2.889 to 2.936 Å (2.8959(8)–2.9605(8) Å in [Se-$(AuPPh_3)_4](OTf)_2$. The Se–Au distances (from 2.492 to 2.511 Å) also compare well with those obtained for [Se-$(AuPPh_3)_4](OTf)_2$ (2.4654(13)–2.54347(14) Å). The cations are paired across symmetry centers to form loose dimers (Figure 5). The shortest intercation distances (Au1···Au4a = 3.298 Å) are similar in length to the Se···Au3′ contacts found for the dimers in $[Se(AuPPh_3)_4]$-$(OTf)_2$. This is the main difference between the two structures, and **14** thus resembles more closely the triply bridging selenido compounds $[Se(AuPPh_3)_3]OTf$ and $[Se(Au_2dppf)\{Se(Au_2dppf)\}_2](OTf)_2$ (**13**), in which

Table 3. Selected Bond Lengths [Å] and Angles [deg] for Compound 13

Au(1)−P(1)	2.277(2)	Au(6)−Se(2)	2.4658(9)
Au(1)−Se(1)	2.4420(9)	Au(3)−Se(1)	2.4704(10)
Au(1)−Au(2)	3.1514(6)	Au(3)−Au(6)	2.9779(6)
Au(1)−Au(4)	3.3392(5)	Au(3)−Au(4)	3.0088(5)
Au(1)−Au(3)	3.3775(6)	Au(4)−P(4)	2.259(3)
Au(2)−P(2)	2.269(3)	Au(4)−Se(1)	2.4240(10)
Au(2)−Se(2)	2.4487(10)	Au(5)−P(5)	2.262(3)
Au(2)−Au(6)	3.1512(5)	Au(5)−Se(2)	2.4474(10)
Au(2)−Au(5)	3.4325(6)	Au(5)−Au(6)	2.9028(5)
Au(3)−P(3)	2.280(3)	Au(6)−P(6)	2.267(2)
P(1)−Au(1)−Se(1)	172.53(7)	P(5)−Au(5)−Au(6)	123.48(6)
P(1)−Au(1)−Au(2)	104.70(6)	Se(2)−Au(5)−Au(6)	54.08(2)
Se(1)−Au(1)−Au(2)	80.86(2)	P(5)−Au(5)−Au(2)	141.42(7)
P(1)−Au(1)−Au(4)	128.63(6)	Se(2)−Au(5)−Au(2)	45.50(2)
Se(1)−Au(1)−Au(4)	46.44(2)	Au(6)−Au(5)−Au(2)	58.951(12)
Au(2)−Au(1)−Au(4)	126.546(14)	P(6)−Au(6)−Se(2)	172.29(6)
P(1)−Au(1)−Au(3)	137.29(7)	P(6)−Au(6)−Au(5)	118.91(6)
Se(1)−Au(1)−Au(3)	46.92(2)	Se(2)−Au(6)−Au(5)	53.49(2)
Au(2)−Au(1)−Au(3)	86.748(13)	P(6)−Au(6)−Au(3)	103.49(6)
Au(4)−Au(1)−Au(3)	53.222(11)	Se(2)−Au(6)−Au(3)	83.57(3)
P(2)−Au(2)−Se(2)	164.40(7)	Se(2)−Au(6)−Au(2)	49.88(2)
P(2)−Au(2)−Au(6)	136.88(6)	Au(5)−Au(6)−Au(2)	68.939(13)
Se(2)−Au(2)−Au(6)	50.36(2)	Au(3)−Au(6)−Au(2)	94.074(14)
P(2)−Au(2)−Au(1)	102.73(6)	Au(4)−Se(1)−Au(1)	86.66(3)
Se(2)−Au(2)−Au(1)	90.47(3)	Au(4)−Se(1)−Au(3)	75.86(3)
Au(6)−Au(2)−Au(1)	88.754(13)	Au(1)−Se(1)−Au(3)	86.87(3)
P(2)−Au(2)−Au(5)	123.80(6)	Au(5)−Se(2)−Au(2)	89.02(3)
Se(2)−Au(2)−Au(5)	45.47(2)	Au(5)−Se(2)−Au(6)	72.43(3)
Au(6)−Au(2)−Au(5)	52.110(11)	Au(2)−Se(2)−Au(6)	79.76(3)
Au(1)−Au(2)−Au(5)	132.605(16)	C(131)−P(5)−Au(5)	116.7(3)
P(3)−Au(3)−Se(1)	172.19(7)	C(111)−P(5)−Au(5)	112.6(3)
P(3)−Au(3)−Au(6)	115.31(6)	C(121)−P(5)−Au(5)	108.7(4)
Se(1)−Au(3)−Au(6)	72.49(2)	C(51)−P(3)−Au(3)	110.0(3)
P(3)−Au(3)−Au(4)	120.91(6)	C(81)−P(3)−Au(3)	117.0(3)
Se(1)−Au(3)−Au(4)	51.37(2)	C(71)−P(3)−Au(3)	112.3(3)
Au(6)−Au(3)−Au(4)	122.876(16)	C(6)−P(2)−Au(2)	111.1(3)
P(3)−Au(3)−Au(1)	131.69(6)	C(31)−P(2)−Au(2)	107.1(3)
Se(1)−Au(3)−Au(1)	46.21(2)	C(41)−P(2)−Au(2)	120.9(3)
Au(6)−Au(3)−Au(1)	87.589(14)	C(1)−P(1)−Au(1)	111.5(3)
Au(4)−Au(3)−Au(1)	62.736(12)	C(21)−P(1)−Au(1)	117.1(3)
P(4)−Au(4)−Se(1)	174.68(7)	C(11)−P(1)−Au(1)	111.5(3)
P(4)−Au(4)−Au(3)	122.35(6)	C(56)−P(4)−Au(4)	107.9(3)
Se(1)−Au(4)−Au(3)	52.77(2)	C(91)−P(4)−Au(4)	113.1(3)
P(4)−Au(4)−Au(1)	130.55(6)	C(101)−P(4)−Au(4)	115.1(3)
Se(1)−Au(4)−Au(1)	46.89(2)	C(116)−P(6)−Au(6)	109.6(3)
Au(3)−Au(4)−Au(1)	64.042(12)	C(141)−P(6)−Au(6)	113.2(3)
P(5)−Au(5)−Se(2)	172.17(8)	C(151)−P(6)−Au(6)	111.8(3)

the selenium−selenium distances are longer than gold−gold distances when considering two "SeAu₃" cores.

Theoretical Calculations

The compounds described in the Experimental Section present short Au(I)−Au(I) contacts. To understand their origin, we have carried out ab initio calculations at MP2 and HF levels with quasi-relativistic pseudopotentials (Table 4). The computational details are described in the molecular orbital calculations section. The total energies and optimized geometries are shown in Tables 5 and 6, respectively. Geometries of the $[Se(AuPH_3)_n]^{(n-2)+}$ ($n = 2-6$) models are illustrated in Figure 5. The results indicate that the various structural parameters change substantially when they are compared at the HF and MP2 levels; the gold−gold distances are significantly shortened and Au−Se−Au angles narrowed for the latter method and are comparable in magnitude with known experimental values (see Table 6). This gives some impression of the contribution of electron correlation to the intramolecular contacts for these clusters. Since it has been suggested that aurophilic attraction is primarily a correlation effect, the HF calculations provide a convenient way of turning off the attraction.[6]
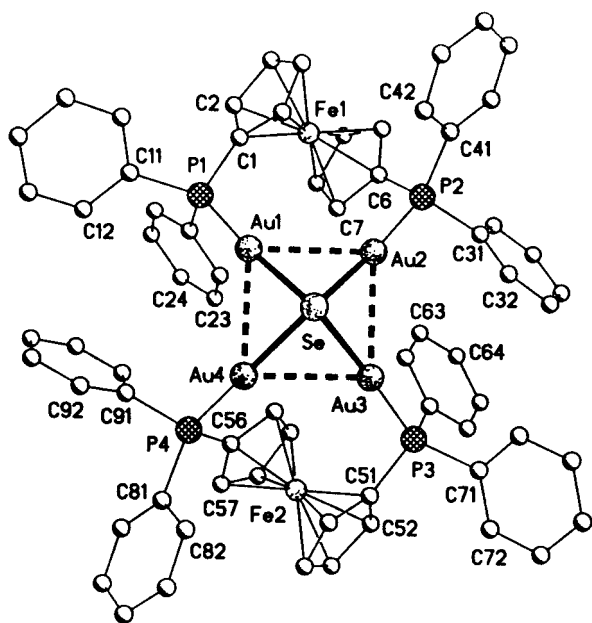
Figure 4. Structure of the cation of complex **14** in the crystal.
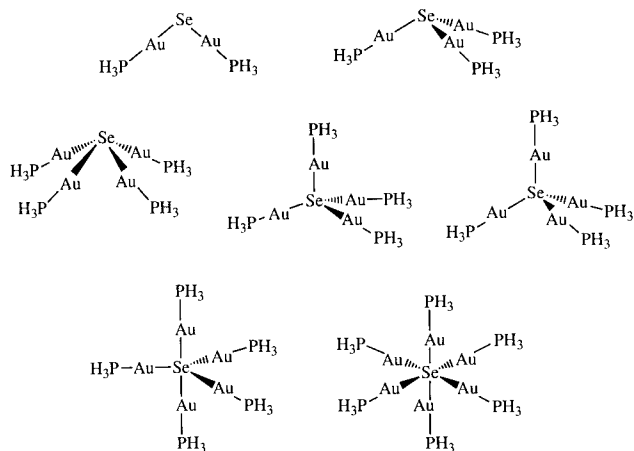
Figure 5. Geometries of the $[Se(AuPH_3)_n]^{(n-2)+}$ ($n = 2-6$) models.

There exists theoretical evidence indicating that the MP2 method may exaggerate the aurophilic attraction.[2] A more exact method would be CCSD (coupled cluster single and double), but it is very expensive for a study of this magnitude of the systems in which we are interested.

For the systems with $n = 4$ and 5, various geometrical arrangements of the $(AuPH_3)$ fragments are possible around the central Se atom. It is a well-known principle in coordination chemistry that systems of the type ML_n prefer a tetrahedral geometry for $n = 4$, whereas trigonal bipyramids are typical for $n = 5$. Systems analogous to the ours, such as $[X(AuL)_n]^{m+}$ ($X = C$, N, O, S, P; $n = 3-6$), have previously been studied by Pyykkö *et al.*,[12] establishing that when attractive forces are present between the $-AuPH_3$ fragments, deviations from the ideal structure must be expected. Thus, the tetrahedral symmetry was lowered to C_{4v}, resulting in four Au−Au distances shorter than in the tetrahedral case. In the pentacoordinated case, a C_{3v} arrangement of the ligands is preferred over the C_s structure.

(12) Pyykkö, P.; Tamm, T. *Organometallics* **1998**, *17*, 4842.

atom PP	basis	remarks
H −	(4s1p)/[2s1p]	$\alpha_p = 0.80$[21]
P Bergner 5-VE	(4s4p1d)/[2s2p1d]	$\alpha_d = 0.34$
Se Bergner 6-VE	(4s4p1d)/[2s2p1d]	$\alpha_d = 0.25$
Au Andrae 19-VE	(8s6p5d1f)/[6s5p3d1f]	$\alpha_f = 0.20$

Table 5. Total Energies of the Systems (in au)

system	Hartree−Fock	MP2
$Se(AuPH_3)_2$ C_{2v}	−295.346744	−296.185816
$Se(AuPH_3)_3^+$ C_{3v}	−438.300352	−439.484695
$Se(AuPH_3)_4^{2+}$ T_d	−581.133855	−582.618990
$Se(AuPH_3)_4^{2+}$ C_{3v}	−581.133855	−582.621580
$Se(AuPH_3)_4^{2+}$ C_{4v}	−581.104087	−582.642334
$Se(AuPH_3)_5^{3+}$ C_{3v}	−723.117459	−724.916119
$Se(AuPH_3)_5^{3+}$ C_s	−723.111230	−724.913063
$Se(AuPH_3)_6^{4+}$ D_{3d}	−867.632215	−868.524890

The relevant experimental structural data are included in Table 6. We have taken the average crystallographic angles and distances for these systems.[9−11] It should be mentioned that at the experimental level the −PPh$_3$ groups are replaced by −PH$_3$ and the ferrocene bridged ligands by −H.

Se(AuPH_3)_2. This system has also been studied theoretically by Pyykkö et al.,[13] who found a gold−gold contact when their MP2 calculations included electronic correlation and quasi-relativistic effects. The difference between the previous calculations and ours (Table 6) is that we have fully optimized the structure. However, both calculations generate an Au−Se−Au angle and Au−Au distance very similar at the MP2 level, 75.4°, 74.4°, 292 pm, and 295 pm, respectively. At the HF level the angles and distances are appreciably larger.

Se(AuPH_3)_3^+. In this cluster too, when the electronic correlation at the MP2 level is taken into account, the values of the distances and angles approach the experimental data. However, the calculated Au- -Au distances and Au−Se−Au angles are smaller than experimental values, because the MP2 level exaggerates the aurophilic attractions, as for the previous neutral A-frame.[12] On the other hand, the wider bond angles in the experimental system may be caused by steric effects between bulky phenyl groups. There exist for some similar systems (e.g., $X(AuPH_3)_3^+$, $X = O$, S),[8d] calculations based on density functional theory (DFT) with electronic correlation and relativistic effects. However, they are not as consistent with the experimental data, being instead comparable to Hartree−Fock calculations. This is because the density functional calculations are unable to describe van der Waals interactions among metallic centers; such interactions are not related in any simple way to the electron density.[3]

Se(AuPH_3)_4^{2+}. C_{4v}, C_{3v}, and T_d relative MP2 energies are 0, +54, +61 kJ/mol. This order rationalizes for the first time the observed C_{4v} structure,[9] and shows that the geometry adopted by the cluster is directly related to the van der Waals interactions established between the gold centers (MP2) and the number of these, with a maximum for the structure with C_{4v} symmetry. If we compare the relative energies at the HF level, we find the opposite trend (see Table 5).

Se(AuPH_3)_5^{3+}. For this type of cluster a trigonal bipyramidal C_{3v} (distorted D_{3h}) symmetry is preferred

(13) Li, J.; Pyykkö, P. *Chem. Phys. Lett.* **1992**, *197*, 586.

Table 6. Main Geometric Parameters of the Selenium Centered Systems (in pm and degrees).

system	method	Se−Au bond	Au···Au distance	Au−P bond	Au−Se−Au angle
[Se(AuPPh$_3$)$_2$]	expt[11]	239.4	305.1	225.4	79.1
[Se(AuPH$_3$)$_2$] C_{2v}	HF	245.7	363.7	241.5	95.49
	MP2	241.9	292.4	231.5	74.36
[Se(AuPPh$_3$)$_3$]PF$_6$	expt[10]	244.7	301.8	227.4	80.1
[Se(AuPH$_3$)$_3$]$^+$ C_{3v}	HF	250.4	385.0	241.5	100.5
	MP2	246.5	297.5	232.5	74.2
[Se(AuPPh$_3$)$_4$](CF$_3$SO$_3$)$_2$	expt[9]	249.5	292.5	227	71.52
[Se(AuPH$_3$)$_4$]$^{2+}$ T_d	HF	254.7	415.8	241.3	109.5
	MP2	243.8	398.1	232.3	109.5
[Se(AuPH$_3$)$_4$]$^{2+}$ C_{3v}	HF	254.6	415.7a	241.3	109.42[a]
	MP2	247.6	350a-429[b]	234.9	90.4[a]–125[b]
[Se(AuPH$_3$)$_4$]$^{2+}$ C_{4v}	HF	258.9	333.8	241.9	80.24
	MP2	247.6	288.8	234.9	71.36
[Se(AuPH$_3$)$_5$]$^{3+}$ C_{3v}	HF	261[a]	451[a]	240[a]	120[d]
		267[c]	373[b]	240[c]	90[b]
	MP2	246[a]	423[d]	230[a]	120[d]
		248[c]	348[b]	232[c]	90[b]
[Se(AuPH$_3$)$_5$]$^{3+}$ C_s	HF	262[c]	453[f]	240[a]	116.4[f]
		266[e]	363[e]	240[c]	82.3[b]
	MP2	243[c]	433[d]	230[a]	118.3[d]
		247[e]	352[b]	232[c]	80.2[b]
[Se(AuPH$_3$)$_6$]$^{4+}$ D_{3d}	HF	268	354	240	90.0
	MP2	248	302	232	90.0

[a] Equatorial. [b] Axial to equatorial. [c] Axial. [d] Equatorial to equatorial. [e] Nonaxial. [f] Axial to nonaxial.

over the C_s (C_{4v} for the Se−Au core) by 8 kJ/mol (at the MP2 level). For this system it has not been possible to obtain the X-ray structure, but the geometry is analogous with that for the carbon derivatives.[12] Our calculations serve as a prediction of the geometry of the selenium compounds.

Se(AuPH$_3$)$_6^{4+}$. The structural framework is calculated to display octahedral geometry (distorted D_{3h} symmetry). Again it has not been possible to determine its X-ray structure. Due to the effect of the electronic correlation at the MP2 level, the Au−Se and Au−Au distances are shorter than at the HF level (see Table 6).

Conclusions

Several gold compounds with a central selenium atom have been prepared and characterized. They show unusual geometries with short gold−gold interactions. Theoretical calculations at the MP2 level with quasi-relativistic pseudopotentials are in agreement with experimental geometries. We attribute the change in the ideal geometry of the compounds to the presence of strong Au···Au interactions that contribute to the stabilization of the different compounds.

Experimental Section

Instrumentation. Infrared spectra were recorded in the range 4000−200 cm^{-1} on a Perkin-Elmer 883 spectrophotometer using Nujol mulls between polyethylene sheets. Conductivities were measured in ca. 5×10^{-4} mol dm^{-3} solutions with a Philips 9509 conductimeter. C, H, and S analyses were carried out with a Perkin-Elmer 2400 microanalyzer. Mass spectra were recorded on a VG Autospec, with the liquid secondary-ion mass spectra (LSIMS) technique, using nitrobenzyl alcohol as matrix. NMR spectra were recorded on a Varian Unity 300 spectrometer and a Bruker ARX 300 spectrometer in CDCl$_3$ (otherwise stated). Chemical shifts are cited relative to SiMe$_4$ (^{1}H, external) and 85% H$_3$PO$_4$ (^{31}P, external).

Materials. The starting materials [Se(AuPPh$_3$)$_2$],[11] [Au$_2$Cl$_2$-(μ-dppf)],[14] and [Au(tht)$_2$]ClO$_4$[15] were prepared by published procedures. [Au(OTf)(PPh$_3$)] was prepared from [AuCl(PPh$_3$)][16] by reaction with AgOTf in dichloromethane; [Au$_2$(OTf)$_2$(μ-dppf)] from [Au$_2$Cl$_2$(μ-dppf)] and 2 equiv of AgOTf in dichloromethane.

Safety Note. Caution! Perchlorate salts of metal complexes with organic ligands are potentially explosive. Only small amounts of material should be prepared, and these should be handled with great caution.

Synthesis of [Se(AuPPh$_3$)$_n$](OTf)$_{n-2}$ ($n = 3$ (**2**), 4 (**3**), 5 (**4**), 6 (**5**)). To a solution of [Se(AuPPh$_3$)$_2$] (0.100 g, 0.1 mmol) in 20 mL of dichloromethane was added the corresponding amount of [Au(OTf)PPh$_3$] (0.061 g, 0.1 mmol, **2**; 0.122 g, 0.2 mmol, **3**; 0.183 g, 0.3 mmol, **4**; 0.244 g, 0.4 mmol, **5**) and the mixture stirred for 15 min. Concentration of the solution to ca. 5 mL and addition of hexane (10 mL) gave complex **2**, **3**, **4**, or **5** as a white solid. Complex **2**: yield 85%; Λ_M 102 Ω^{-1} cm^2 mol^{-1}. Anal. Found: C, 41.23; H, 2.76; S, 2.14. Calcd for C$_{55}$H$_{45}$-Au$_3$F$_3$O$_3$P$_3$SSe: C, 41.12; H, 2.80; S, 1.99. NMR data. ^{31}P(^{1}H), δ: 34.7 (s) ppm. Complex **3**: yield 81%; Λ_M 165 Ω^{-1} cm^2 mol^{-1}. Anal. Found: C, 39.65; H, 2.71; S, 2.42. Calcd for C$_{74}$H$_{60}$-Au$_4$F$_6$O$_6$P$_4$S$_2$Se: C, 40.12; H, 2.71; S, 2.84. ^{31}P(^{1}H), δ: 33.5 (s) ppm. Complex **4**: yield 76%; Λ_M 293 Ω^{-1} cm^2 mol^{-1}. Anal. Found: C, 39.02; H, 2.55; S, 3.91. Calcd for C$_{93}$H$_{75}$Au$_5$F$_9$O$_9$P$_5$S$_3$-Se: C, 39.56; H, 2.66; S, 3.40. ^{31}P(^{1}H), δ: 32.6 (s) ppm. Complex **5**: yield 71%; Λ_M 350 Ω^{-1} cm^2 mol^{-1}. Anal. Found: C, 39.55; H, 2.38; S, 2.57. Calcd for C$_{112}$H$_{90}$Au$_6$F$_{12}$O$_{12}$P$_6$S$_4$Se: C, 39.19; H, 2.62; S, 3.23. ^{31}P(^{1}H), δ: 31.7 (s) ppm.

Synthesis of [Au{Se(AuPPh$_3$)$_2$}$_2$]ClO$_4$, 6. To a solution of [Se(AuPPh$_3$)$_2$] (0.200 g, 0.2 mmol) in 20 mL of dichloromethane was added [Au(tht)$_2$]ClO$_4$ (0.047 g, 0.1 mmol), and the mixture was stirred for 30 min. Evaporation of the solvent to ca. 5 mL and addition of diethyl ether (10 mL) gave a white solid of complex **6**. Yield: 57%; Λ_M 95 Ω^{-1} cm^2 mol^{-1}. Anal. Found: C, 38.11; H, 2.61. Calcd for C$_{72}$H$_{60}$Au$_5$ ClO$_4$P$_4$Se$_2$: C, 37.72; H, 2.62. ^{31}P(^{1}H), δ: 35.3 (s) ppm.

Synthesis of [Se(Au$_2$dppf)], 7. To a solution of [Au$_2$Cl$_2$-(μ-dppf)] (1.019 g, 1 mmol) in 20 mL of acetone was added a

(14) Gimeno, M. C.; Laguna, A.; Sarroca, C.; Jones, P. G. *Inorg. Chem.* **1993**, *32*, 5926.
(15) Usón, R.; Laguna, A.; Laguna, M.; Jiménez, J.; Gómez M. P.; Sainz, A.; Jones, P. G. *J. Chem. Soc., Dalton Trans.* **1990**, 3457.
(16) Usón, R.; Laguna, A. *Inorg. Synth.* **1982**, *21*, 71.

Table 7. Details of Data Collection and Structure Refinement for Complexes 7, 12b, and 13

	7	12b·8CH₂Cl₂	13·3.5CH₂Cl₂
chemical formula	$C_{34}H_{28}Au_2FeP_2Se$	$C_{144}H_{128}Au_{10}Cl_{16}Fe_4N_2O_6P_8Se_4$	$C_{107.5}H_{91}Au_6Cl_7Fe_6O_6S_2Se_2$
cryst habit	yellow prism	yellow tablet	yellow plate
cryst size/mm	$0.32 \times 0.18 \times 0.15$	$0.28 \times 0.17 \times 0.10$	$0.25 \times 0.16 \times 0.08$
cryst syst	monoclinic	monoclinic	monoclinic
space group	$P2_1/c$	$C2/c$	$P2_1/n$
$a/Å$	10.942(2)	34.142(7)	20.5931(18)
$b/Å$	15.816(2)	22.064(5)	19.5047/16
$c/Å$	18.066(3)	24.354(5)	28.984(2)
β/deg	104.030(14)	118.695(9)	102.814(3)
$U/Å^3$	3033.4(8)	16093(6)	11351.7(17)
Z	4	4	4
D_c/g cm^{-3}	2.249	2.190	2.105
M	1027.25	5306.35	3598.16
$F(000)$	1920	9904	6796
T/°C	-100	-130	-130
$2\theta_{max}$/deg	50	50	52
μ(Mo Kα)/cm^{-1}	115	107	91
transmission	0.890−0.775	0.801−0.350	0.802−0.389
no. of reflns measd	5385	46 530	115 873
no. of unique reflns	5319	14 132	23 217
R_{int}	0.078	0.212	0.108
R^a ($F>4\sigma(F)$)	0.0382	0.1115	0.0438
wR^b (F^2, all reflns)	0.0793	0.3442	0.1049
no. of reflns used	5319	14 132	23 217
no. of params	362	306	1224
no. of restraints	316	13	263
S^c	0.865	0.975	0.949
max. $\Delta\rho$/e Å^{-3}	1.877	4.877	2.224

^{a} $R(F)= \Sigma||F_o| - |F_c||/\Sigma|F_o|$. ^{b} $wR(F^2) = [\Sigma\{w(F_o^2 - F_c^2)2\}/\Sigma\{w(F_o^2)^2\}]^{0.5}$; $w^{-1} = \sigma^2(F_o^2) + (aP)^2 + bP$, where $P = [F_o^2 + 2F_c^2]/3$ and a and b are constants adjusted by the program. ^{c} $S = [\Sigma\{w(F_o^2 - F_c^2)^2\}/(n - p)]^{0.5}$, where n is the number of data and p the number of parameters.

solution of SeC(NH₂)₂ (0.123 g, 1 mmol) in acetone (20 mL) and the mixture stirred for 1 h. The white precipitate formed was filtered off, then dissolved in 10 mL of methanol, and a solution of Na₂CO₃ in water was added. The mixture was stirred for 4 h and then washed with CH₂Cl₂. The organic phase was separated and dried with MgSO₄. Evaporation of the solvent and addition of diethyl ether gave an orange solid of complex **7**. Yield: 45%; Λ_M 0.6 Ω⁻¹ cm² mol⁻¹. Anal. Found: C, 39.5; H, 2.5. Calcd for C₃₄H₂₈Au₂FeP₂Se: C, 39.7; H, 2.7. ³¹P(¹H), δ: 31.4 (s) ppm; ¹H, δ: 3.89 (m, 4H, C₅H₄), 5.27 (m, 4H, C₅H₄), 7.4−7.6 (m, 20H, Ph).

Synthesis of [Se(Au₂dppf)(AuPR₃)]OTf (PR₃ = PPh₃ 8, PPh₂Me 9). To a solution of complex **7** (0.102 g, 0.1 mmol) in 20 mL of dichloromethane was added [Au(OTf)PPh₃] (0.061 g, 0.1 mmol) or [Au(OTf)PPh₂Me] (0.054 g, 0.1 mmol) and the mixture stirred for 1 h. Evaporation of the solvent to ca. 5 mL and addition of hexane afforded orange solids of complexes **8** and **9**, respectively. Complex **8**: Yield 80%; Λ_M 98 Ω⁻¹ cm² mol⁻¹. Anal. Found: C, 38.89; H, 2.55; S, 2.10. Calcd for C₅₃H₄₃Au₃F₃FeO₃P₃SSe: C, 38.82; H, 2.80; S, 1.95. ³¹P(¹H), δ: 29.3 (s, 2P, dppf), 35.9 (s, 1P, PPh₃) ppm; ¹H, δ: 4.08 (m, 4H, C₅H₄), 4.45 (m, 4H, C₅H₄), 7.3−7.5 (m, 35H, Ph). Complex **9**: Yield 83%; Λ_M 102 Ω⁻¹ cm² mol⁻¹. Anal. Found: C, 36.16; H, 2.62; S, 1.96. Calcd for C₄₈H₄₁Au₃F₃FeO₃P₃SSe: C, 36.62; H, 2.61; S, 2.03. ³¹P(¹H), δ: 28.7 (s, 2P, dppf), 21.2 (s, 1P, PPh₂Me) ppm. ¹H, δ: 4.06 (m, 4H, C₅H₄), 4.50 (m, 4H, C₅H₄), 7.2−7.6 (m, 30H, Ph).

Synthesis of [Se(Au₂dppf)(AuPR₃)₂](OTf)₂ (PR₃ = PPh₃ 10, PPh₂Me 11). To a solution of complex **7** (0.102 g, 0.1 mmol) in 20 mL of dichloromethane was added [Au(OTf)PPh₃] (0.122 g, 0.2 mmol) or [Au(OTf)PPh₂Me] (0.108 g, 0.2 mmol) and the mixture stirred for 1 h. Evaporation of the solvent to ca. 5 mL and addition of hexane afforded orange solids of complexes **10** and **11**, respectively. Complex **10**: Yield 55%; Λ_M 150 Ω⁻¹ cm² mol⁻¹. Anal. Found: C, 38.89; H, 2.40; S, 3.07. Calcd for C₇₂H₅₈Au₄F₆FeO₆P₄S₂Se: C, 38.58; H, 2.58; S, 2.85. ³¹P(¹H), δ: 28.0 (s, 2P, dppf), 31.1 (s, 2P, PPh₃) ppm. ¹H, δ: 4.18 (m, 4H, C₅H₄), 4.60 (m, 4H, C₅H₄), 7.3−7.6 (m, 50H, Ph). Complex **11**: Yield 76%; Λ_M 156 Ω⁻¹ cm² mol⁻¹. Anal. Found: C, 34.76; H, 2.64;

S, 2.93. Calcd for C₆₂H₅₄Au₄F₆FeO₆P₄S₂Se: C, 35.11; H, 2.54; S, 3.02. ³¹P(¹H), δ: 28.5 (s, 2P, dppf), 20.7 (s, 2P, PPh₂Me) ppm. ¹H, δ: 4.11 (m, 4H, C₅H₄), 4.57 (m, 4H, C₅H₄), 7.2−7.8 (m, 40H, Ph).

Synthesis of [Au{Se(Au₂dppf)}₂]ClO₄, 12a. To a solution of complex **7** (0.204 g, 0.2 mmol) in 20 mL of dichloromethane was added [Au(tht)₂]ClO₄ (0.047 g, 0.1 mmol) and the mixture stirred for 30 min. Evaporation of the solvent to ca. 5 mL and addition of ca. 10 mL of diethyl ether gave a yellow solid of complex **12a**: Yield 93%; Λ_M 110 Ω⁻¹ cm² mol⁻¹. Anal. Found: C, 34.27; H, 2.32. Calcd for C₆₈H₅₆Au₅ClFe₂O₄P₄Se₂: C, 34.72; H, 2.38. ³¹P(¹H), rt, δ: 28.2 (br, 4P, dppf) ppm. ¹H, rt, δ: 4.4 (m, br, 8H, C₅H₄), 4.7 (m, br, 8H, C₅H₄), 7.2−7.6 (m, 40H, Ph). ³¹P(¹H), −55 °C, δ: 21.5 (s, 1P, dppf), 23.5 (s, 1P, dppf), 26.0 (s, 1P, dppf), 27.3 (s, 1P, dppf) ppm. ¹H, −55 °C., δ: 3.34 (m, 1H, C₅H₄), 3.43 (m, 1H, C₅H₄), 3.58 (m, 1H, C₅H₄), 3.69 (m, H, C₅H₄), 3.79 (m, 1H, C₅H₄), 4.05 (m, 1H, C₅H₄), 4.20 (m, 1H, C₅H₄), 4.26 (m, 1H, C₅H₄), 4.33 (m, 1H, C₅H₄), 4.40 (m, 1H, C₅H₄), 4.71 (m, 1H, C₅H₄), 4.80 (m, 1H, C₅H₄), 5.01 (m, 1H, C₅H₄), 5.48 (m, 1H, C₅H₄), 5.58 (m, 1H, C₅H₄), 6.8−8.2 (m, 60H, Ph).

Synthesis of [(Au₂dppf){Se(Au₂dppf)}₂](OTf)₂, 13. To a solution of complex **7** (0.204 g, 0.2 mmol) in 20 mL of dichloromethane was added [Au₂(OTf)₂(μ-dppf)] (0.124 g, 0.1 mmol) and the mixture stirred for 30 min. Evaporation of the solvent to ca. 5 mL and addition of ca. 10 mL of hexane gave an orange solid of complex **13**: Yield 66%; Λ_M 170 Ω⁻¹ cm² mol⁻¹. Anal. Found: C, 37.46; H, 2.38; S, 1.71. Calcd for C₁₀₄H₈₄Au₆F₆Fe₃O₆P₆S₂Se₂: C, 37.09; H, 2.54; S, 1.93. ³¹P(¹H), rt, δ: 28 (br, 6P, dppf) ppm. ¹H, rt, δ: 4.43 (m, br, 16H, C₅H₄), 7.2−7.8 (m, 60H, Ph). ³¹P(¹H), −55 °C, δ: 22.8 (s, 2P, dppf), 26.9 (s, 2P, dppf), 29.0 (s, 2P, dppf) ppm. ¹H, −55 °C, δ: 4.06 (m, 2H, C₅H₄), 4.15 (m, 2H, C₅H₄), 4.40 (m, 4H, C₅H₄), 4.51 (m, 8H, C₅H₄), 4.65 (m, 4H, C₅H₄), 6.8−8.2 (m, 60H, Ph).

Synthesis of [Se(Au₂dppf)₂](OTf)₂, 14. To a solution of complex **7** (0.102 g, 0.1 mmol) in 20 mL of dichloromethane was added [Au₂(OTf)₂(μ-dppf)] (0.124 g, 0.1 mmol) and the mixture stirred for 30 min. Then the solvent was evaporated to ca. 5 mL, and addition of hexane gave an orange solid of

complex **14**: Yield 75%; Λ_M 160 Ω^{-1} cm^2 mol^{-1}. Anal. Found: C, 36.66; H, 2.40; S, 2.32. Calcd for $C_{70}H_{56}Au_4F_6Fe_2O_6P_4S_2Se$: C, 36.96; H, 2.46; S, 2.80. ^{31}P(^{1}H), rt, δ: 28.3 (br, 4P, dppf) ppm. ^{1}H, rt, δ: 4.3 (m, br, 8H, C_5H_4), 4.5 (m, br, 8H, C_5H_4), 7.4−7.8 (m, 40H, Ph). ^{31}P(^{1}H), −55 °C, δ: 22.8 (s, 2P, dppf, **13**), 26.9 (s, 2P, dppf, **13**), 29.0 (s, 2P, dppf, **13**), 27.8 (s, 4P, dppf, **14**), 30.0 (s, 2P, dppf) ppm. ^{1}H, −55 °C, δ: 3.6−5.0 (m, br, C_5H_4), 6.6−8.2 (m, Ph).

Synthesis of [Se(Au$_2$dppf)$_3$](OTf)$_4$, 15. To a solution of complex **7** (0.102 g, 0.1 mmol) in 20 mL of dichloromethane was added [Au$_2$(OTf)$_2$(μ-dppf)] (0.249 g, 0.2 mmol) and the mixture stirred for 30 min. Then the solvent was evaporated to ca. 5 mL, and addition of hexane gave an orange solid of complex **15**: Yield 73%; Λ_M 340 Ω^{-1} cm^2 mol^{-1}. Anal. Found: C, 36.03; H, 2.46; S, 3.07. Calcd for $C_{106}H_{84}Au_6F_{12}Fe_3O_{12}P_6S_4$-Se: C, 36.15; H, 2.38; S, 3.63. ^{31}P(^{1}H), rt, δ: 27.6 (s, 6P, dppf) ppm. ^{1}H, rt, δ: 4.47 (m, br, 24H, C_5H_4), 7.3−7.6 (m, 60H, Ph). ^{31}P(^{1}H), −55 °C, δ: 26.3 (s, dppf), 27.2 (s, dppf), 27.8 (s, dppf), 31.3 (s, dppf) ppm. ^{1}H, −55 °C, δ: 4.16 (m, 8H, C_5H_4), 4.56 (m, 8H, C_5H_4), 4.67 (m, 4H, C_5H_4), 5.13 (m, 4H, C_5H_4), 6.6−8.0 (m, 60H, Ph).

Crystal Structure Determinations. The crystals were mounted in inert oil on glass fibers and transferred to the cold gas stream of a Siemens P4 (**7**) or Bruker SMART diffractometer. Data were collected using monochromated Mo Kα radiation (λ = 0.71073 Å) in ω-scan mode. An absorption correction was applied on the basis of ψ-scans for **7**, whereas for **12b**−**14** the program SADABS, based on multiple scans, was used. The structures were solved by direct methods and refined on F^2 using the program SHELXL-97.[17] All non-hydrogen atoms were refined anisotropically except for solvent. Hydrogen atoms were included using a riding model. Further crystal data are given in Table 7. *Special details of refinement*: Compound **12b**: The structure contains extensive

(17) Sheldrick, G. M. *SHELXL-97*, a program for crystal structure refinement; University of Göttingen, Germany, 1997.
(18) Frisch, M. J.; Trucks, G. W.; Schlegel, H. B.; Gill, P. M. W.; Johnson, B. G.; Robb, M. A.; Cheeseman, J. R.; Keith, K. T.; Petersson, G. A.; Montgomery, J. A.; Raghavachari, K.; Al-Laham, M. A.; Zakrzewski, V. G.; Ortiz, J. V.; Foresman, J. B.; Cioslowski, J.; Stefanov, B. B.; Nanayakkara, A.; Challacombe, M.; Peng, C. Y.; Ayala, P. Y.; Chen, W.; Wong, M. W.; Andres, J. L.; Replogle, E. S.; Gomperts, R.; Martin, R. L.; Fox, D. J.; Binkley, J. S.; Defrees, D. J.; Baker, J.;. Stewart, J. P.; Head-Gordon, M.; Gonzalez, C.; Pople, J. A. *Gaussian 98*; Gaussian, Inc.: Pittsburgh, PA, 1998.
(19) Andrae, D.; Häusserman, M.; Dolg, H.; Stoll, H.; Preuss, H. *Theor. Chim. Acta* **1990**, *77*, 123.
(20) Bergner, A.; Dolg, M.; Küchle, W.; Stoll, H.; Preuss, H. *Mol. Phys.* **1993**, *80*, 1431.
(21) Dunning, T. H.; Hay, P. J. In *Modern Theoretical Chemistry*, Vol. 3 Schaefer, H. F., III, Ed.; Plenum Press: New York, 1997; pp 1−28.

regions of severely disordered dichloromethane which were arbitrarily refined as chlorine sites of varying occupation. The high residuals, associated with this problem, indicate that the structure should be interpreted with caution, but we are confident that its main features are correct. The agreement factors are necessarily poor. The largest residual electron density in this complex is near the gold atoms. Complex **13** crystallizes with four molecules of dichloromethane, of which one was arbitrarily assigned occupancy of 0.5 to obtain reasonable U values.

Molecular Orbital Calculations. The Gaussian 98 package[18] was used. The basis sets and pseudopotentials (PP) used in the production runs are given in Table 4. The 19-valence electron (VE) quasi-relativistic (QR) pseudopotential of Andrae[19] was employed for gold. We have employed one f-type polarization function for Au. The f orbitals are necessary for the weak intermolecular interactions, as was demonstrated previously for different metals.[5] The atoms C, O, P, and Se were also treated by Stuttgart pseudopotentials,[20] including only the valence electron for each atom. For these atoms, double-ζ basis sets were used, augmented by d-type polarization functions. For the H atom, a double-ζ plus one p-type polarization function was used (see Table 1).[21]

We have fully optimized the structures for the models Se(AuPH$_3$)$_2$ (C_{2v}), Se(AuPH$_3$)$_3^+$ (C_{3v}), Se(AuPH$_3$)$_4^{2+}$ (T_d, C_{3v}, C_{4v}), Se(AuPH$_3$)$_5^{3+}$ (C_s), and Se(AuPH$_3$)$_6^{4+}$ (D_{3d}), at Hartree−Fock (HF) and second-order Møller−Plesset perturbation theory (MP2) levels (see Tables 5 and Table 6). In the experimental structures, the ligand on the gold atoms is triphenylphosphine, −P(C$_6$H$_5$)$_3$. This ligand implies a large computational effort; this was replaced by the phosphine group −PH$_3$. If the rotation of the terminal −PH$_3$ ligands would have broken the symmetry, their dihedral angle was fixed.

Supporting Information Available: Three X-ray crystallographic files, in CIF format, for complexes **7**, **12b**, and **13**. This material is available free of charge via the Internet at http://pubs.acs.org.

OM000119G